Proceedings of IMECE2008
2008 ASME International Mechanical Engineering Congress and Exposition
October 31- November 6, 2008, Boston, Massachusetts, USA

IMECE2008-66937

LOCAL GEOMETRIC PROJECTION-BASED NOISE REDUCTION FOR VIBRATION SIGNAL ANALYSIS IN ROLLING BEARINGS

Ruqiang Yan
Dept. of Mechanical & Industrial Engineering
University of Massachusetts
Amherst, MA 01003
E-mail: ryan@ecs.umass.edu

Robert X. Gao*
Dept. of Mechanical & Industrial Engineering
University of Massachusetts
Amherst, MA 01003
E-mail: gao@ecs.umass.edu

Kang B. Lee
Manufacturing Metrology Division
National Institute of Standards and Technology
Gaithersburg, MD 20899
Email: kang.lee@nist.gov

Steven E. Fick
Manufacturing Metrology Division
National Institute of Standards and Technology
Gaithersburg, MD 20899
Email: steven.fick@nist.gov

*Corresponding author: gao@ecs.umass.edu

ABSTRACT

This paper presents a noise reduction technique for vibration signal analysis in rolling bearings, based on local geometric projection (LGP). LGP is a non-linear filtering technique that reconstructs one dimensional time series in a high-dimensional phase space using time-delayed coordinates, based on the Takens embedding theorem. From the neighborhood of each point in the phase space, where a neighbor is defined as a local subspace of the whole phase space, the best subspace to which the point will be orthogonally projected is identified. Since the signal subspace is formed by the most significant eigen-directions of the neighborhood, while the less significant ones define the noise subspace, the noise can be reduced by converting the points onto the subspace spanned by those significant eigen-directions back to a new, one-dimensional time series.

Improvement on signal-to-noise ratio enabled by LGP is first evaluated using a chaotic system and an analytically formulated synthetic signal. Then analysis of bearing vibration signals is carried out as a case study. The LGP-based technique is shown to be effective in reducing noise and enhancing extraction of weak, defect-related features, as manifested by the multifractal spectrum from the signal.

KEYWORDS Local geometric projection, Phase space reconstruction, Noise reduction, Health monitoring

I. INTRODUCTION

Machine condition monitoring and health diagnosis have been an active research area attracting increasing attention from the research community worldwide. Since the occurrence of failures in machine systems is generally accompanied by change of its dynamic characteristics, vibration measurement has been routinely conducted for defect identification. Linear, weak nonlinear or strongly nonlinear behaviors have been observed in vibration signals, reflecting upon the various working conditions of the machines. It was found that non-linear chaotic vibrations were generated in gear systems [1], rolling bearings [2], or generator with a cracked rotor [3]. These observations indicate that non-linear dynamics provide a complementary approach to commonly employed techniques such as spectrum analysis or time-frequency-scale analysis for machine condition monitoring and health diagnosis.

Research on non-linear dynamics has introduced new quantities such as the correlation dimension [4, 5], multifractal spectrum [6], and Lyapunov exponent [7] to interpret signals measured from physical systems where chaotic behaviors are identified. Over the past decade, application of these quantities has been increasingly explored. As an example, correlation dimensions of bearing vibration signals were extracted, and three types of bearing faults were identified from their respective values [4]. The correlation dimension was also able to identify fatigue crack and broken tooth in a gearbox [5]. In another study, the multi-fractal spectrum has shown to be a viable tool for identifying defective machine components [6]. Tao et al. [7] extracted the Lyapunov exponent spectra from vibration signals in order to classify different bearing defects. All of these quantities, however, were found to be sensitive to the presence of noise [8]. Considering that the signal-to-noise

ratio (SNR) of the measured data is low at the early stages of defect inception due to the relatively weak amplitude induced by the defects and structural attenuation between the source of signal generation and the sensor location, it is important to develop noise reduction techniques to maximize the effectiveness of non-linear measures for machine condition monitoring and health diagnosis.

Traditional filters (e.g., low-pass, band-pass, etc.) are effective under conditions where noise component is confined within a known frequency range. As a result, they are generally not effective in reducing the effects of noise in signals in which nonlinear behavior exists. Furthermore, traditional filters may induce distortion because some of the frequency components that characterize the system dynamics can be suppressed by applying these filters. Various studies have been conducted to overcome the difficulty of noise reduction involved in nonlinear behavior [9-14]. For example, a dynamical learning technique was combined with a least-square trajectory procedure to perform noise reduction [10]. A shadowing-based approach was proposed to treat nonlinear chaotic signal [11]. This approach was also integrated with statistical method to achieve comparable denoising results [12]. In another study, local constant fits were used to obtain denoised data in a reconstructed phase space [13]. Cawley and Hsu [14] developed a LGP technique for noise reduction in chaotic maps and flows. Among various approaches described above, the LGP has been investigated by researchers in terms of improving its effectiveness on noise reduction [15, 16], and successfully applied to various problems [17-19]. In an analysis of heart rate variability, it was observed that values of the correlation dimension change after noise reduction [17]. When the LGP method was used for Chinese speech enhancement [18], better performance was shown as compared to two popular algorithms: the E-M and E-V methods. Moreover, weak harmonic signals from chaotic interference were reported to have been extracted using LGP-based noise reduction [19].

This paper investigates the utility of LGP for reducing noise in vibration signals measured on rolling bearings. The paper is organized as follows. Section II introduces the theoretical basis of the LGP algorithm, and considers parameters that determine the effectiveness of the noise reduction algorithm. Section III presents the simulation results using a well-known chaotic system and an analytically formulated synthetic signal, which quantified the signal-to-noise ratio improvement. In section IV, the LGP application to bearing vibration signals is experimentally investigated. Finally, conclusions are drawn in section V.

II. LOCAL GEOMETRIC PROJECTION

Suppose a time series $\{ \bar{x}_1, \bar{x}_2, ..., \bar{x}_N \}$ represents true observable quantities of a given dynamic system. Due to the existence of noise contamination, the measured time series $\{ x_1, x_2, ..., x_N \}$ is expressed as:

$$x_n = \bar{x}_n + \eta_n \qquad n = 1, 2, ..., N \tag{1}$$

where η_n denotes the noise component. The ultimate goal of any noise reduction algorithm is to estimate the time series $\{ \bar{x}_1, \bar{x}_2, ..., \bar{x}_N \}$ from the measured one $\{ x_1, x_2, ..., x_N \}$ such that the following condition is satisfied:

$$\hat{x}_n \approx x_n - \delta x_n \qquad n = 1, 2, ..., N \tag{2}$$

where $\hat{x}_n$ represents the estimation of $\bar{x}_n$ and δx_n denotes the corrections. Combining Eq. (1) with Eq. (2) results in:

$$\hat{x}_n \approx \bar{x}_n + \eta_n - \delta x_n \qquad n = 1, 2, ..., N \tag{3}$$

Equation (3) indicates an ideal noise reduction technique should make the term $\eta_n - \delta x_n$ be equal or close to zero.

The LGP algorithm technique studied in this paper was developed from a phase space perspective, and does not require any prior information on the underlying dynamics of systems being investigated for its implementation [14]. This main idea of the technique is that in a multi-dimensional phase space reconstructed from the measured time series, the true observable quantities and the measurement noise can be decomposed by orthogonal projection into different local subspaces. By rebuilding these local subspaces that are only occupied by those observable quantities, a new time series with the measurement noise removed can be constructed. The four major steps of the process are: 1) phase space reconstruction, 2) neighborhood covering, 3) local subspace projection, and 4) new time series conversion.

Phase Space Reconstruction

In practice, the actual phase space of a dynamic system can seldom be obtained. To solve this problem, the time-delayed coordinates approach based on the Takens embedding theorem [20] is applied to reconstruct the phase space from only one measured time series of the system. For the measured time series $\{ x(1), x(2), ..., x(N) \}$, a series of vectors $X(i)$ in the reconstructed phase space is generated as:

$$\begin{cases} X(1) = \{x(1), x(1+\tau), ..., x(1+(m-1)\tau)\} \\ \quad ... \\ X(i) = \{x(i), x(i+\tau), ..., x(i+(m-1)\tau\} \\ \quad ... \\ X(N-(m-1)\tau) = \{x(N-(m-1)\tau), x(N-(m-2)\tau), ..., x(N)\} \end{cases} \tag{4}$$

where the parameters τ and m are the time delay and the embedding dimension of the reconstructed phase space, respectively. According to the Takens theory [20], a sufficient condition for the embedding dimension is that $m \geq 2d + 1$, where d is the fractal dimension of the analyzed system. Takens also assumed that there are no constraints for the selection of time delay τ if an infinite number of noise-free data points can be obtained. However, since the measured time series only contains a finite number of data points, the time delay τ must be chosen so that the underling dynamics in the reconstructed phase space and the original system are equivalent in the topological sense. Furthermore, the time delay τ can not be

chosen to be too small, as it will make the reconstructed vectors differ insignificantly. On the other hand, if the time delay τ is too large, the time-delay coordinates will be uncorrelated, and will therefore provide no useful information. Various approaches have been developed to determine the parameters τ and *m,* such as the autocorrelation function [9] mutual information [21] for time delay τ, G-P algorithm [22] and False Nearest Neighbors (FNN) [23] for embedding dimension. These approaches assume the selection of the parameters τ and m to be independent. In the present study, the time delay and embedding dimension are determined for the same time using the C-C method based on the concept of the embedding window [24].

Neighborhood Coverage

Subsequent to the phase space reconstruction, a reference point X_1^1 is randomly chosen from all the points $X(i)$ ($i = 1,2,...,N-(m-1)\tau$) as shown in Eq. (4). By finding its *l-1* nearest neighbor points, a neighborhood is formed as:

$$U_1 = \{X_1^1, X_2^1, ..., X_l^1\} \tag{5}$$

where *l* represents the number of points in the neighborhood, and is greater than the embedding dimension *m*.

With the same procedure, the next $N_b - 1$ reference points X_1^h ($h = 2,3,...,N_b$) are selected and subsequently form their corresponding neighborhoods as

$$U_j = \{X_1^j, X_2^j, ..., X_l^j\} \qquad j = 2,3,...N_b \tag{6}$$

It should be noted that the selection of reference point X_1^h is subject to the condition $X_1^h \notin U_k$ ($k = 1,2,...,N_b$) when $h \neq k$. All the N_b locally formulated neighborhoods work together to cover the entire phase space.

Local Subspace Projection

For each neighborhood, the sample average is calculated as:

$$a_k = \sum_{t=1}^{l} X_t^k / l \tag{7}$$

By defining the neighborhood radius as:

$$r_k = \max_{t=1,2,...l} \left\| a_k - X_t^k \right\| \qquad X_t^k \in U_k \tag{8}$$

all the neighborhoods can be reordered as

$$M = \{(X_1^1, U_1), (X_1^2, U_2), ..., (X_1^{N_b}, U_{N_b})\} \tag{9}$$

with increasing r_k. The covariance matrix C_k of the points in each neighborhood is then calculated as:

$$C_k = \frac{1}{l} \sum_{t=1}^{l} [X_t^k - a_k][X_t^k - a_k]^T \tag{10}$$

Performing singular value decomposition on the covariance matrix C_k leads to

$$C_k = A_k \Lambda_k A_k^T \tag{11}$$

where A_k is a $m \times m$ matrix whose columns are orthonormal eigenvectors of the covariance matrix, and $A_k A_k^T = I_m$. The symbol Λ_k denotes a diagonal matrix whose diagonal elements $\lambda_1 \geq \lambda_2 \geq \cdots \geq \lambda_m$ are the eigenvalues of the covariance matrix. Kantz and Schreiber [9] stated that in the *m* dimensional reconstructed phase space, the representation of the underlying dynamics of the system is confined to a low dimensional subspace m_0 ($m_0 < m$). This means there exist $m - m_0$ *null-spaces* in the reconstructed phase space. Any information found in these *null-spaces* must be caused by noise. Therefore, by only projecting the points in the neighborhood into the m_0 subspace, noise can be removed. The projection operator from *m* dimensional phase space to m_0 dimensional subspace is realized as:

$$P_k = B_k B_k^T \tag{12}$$

where B_k is the matrix whose columns are the first m_0 eigenvectors in A_k, which correspond to the largest m_0 eigenvalues of the covariance matrix C_k. All the points in the neighborhood U_k ($k = 1,2,...,N_b$) are replaced by the new adjusted points as

$$\hat{X}_t^k = a_k + P_k(X_t^k - a_k) \qquad t = 1,2,...,l \tag{13}$$

The local subspace projection is performed with the sequence shown in Eq. (9), starting with small neighborhood radius ensures better estimate of underlying dynamics of the system within a local region of the reconstructed phase space [14]. Since each point $\hat{X}_t^k$ has a corresponding one (denoted as a vector) in Eq. (4). The vectors originally generated in the reconstructed phase space shown in Eq. (4) are adjusted as $\hat{X}(i)$ ($i = 1,2,...,N-(m-1)\tau$).

New Time Series Conversion

From the adjusted vectors $\hat{X}(i)$ ($i = 1,2,...,N-(m-1)\tau$), a new time series with noise being removed can be constructed. For the best new time series [14], the minimum error ε is given by:

$$\varepsilon = \min\left(\sum_{i=1}^{N-(m-1)\tau} \sum_{q=1}^{m} \left| \hat{X}_q(i) - \hat{x}(i + (q-1)\tau) \right|^2 \right) \tag{14}$$

where $\hat{X}_q(i)$ denotes the q element in the adjusted vector $\hat{X}(i)$. Accordingly, the new time series is obtained as [14]:

$$\hat{x}(i)=\begin{cases}\frac{1}{s}\sum_{q=1}^{s}\hat{X}_q(i-(q-1)\tau) & 1+(s-1)\tau\le i\le s\tau, s=1,2,...,m-1\\ \frac{1}{m}\sum_{q=1}^{m}\hat{X}_q(i-(q-1)\tau) & 1+(m-1)\tau\le i\le N-(m-1)\tau\\ \frac{1}{s}\sum_{q=m-s+1}^{s}\hat{X}_q(i-(q-1)\tau) & 1+N-s\tau\le i\le N-(s-1)\tau, s=m-1,...,1\end{cases} \quad (15)$$

Quantitative measures can be further extracted from this noise- cleaned time series $\{\hat{x}(1),\hat{x}(2),...,\hat{x}(N)\}$ to characterize the dynamic system being investigated.

III. SIMULATION OF ALGORITHM

To quantitatively evaluate the LGP-based noise reduction algorithm, two simulations were carried out. The first simulation began with a noisy time series generated from a well-known nonlinear dynamic system: the Lorenz system. The second simulation was a time series comprising a series of equally spaced impulsive vibrations, each with a different level of additive white noise.

Lorenz System

The Lorenz system is a typical nonlinear dynamic system derived from simplified equations of atmospheric convection [25], and is expressed as:

$$\begin{cases}\frac{dx}{dt}=\sigma(y-x)\\ \frac{dy}{dt}=\rho x-y-xz\\ \frac{dz}{dt}=-\beta z+xy\end{cases} \quad (16)$$

where σ is the Prandtl number, and ρ is the Rayleigh number. When $\sigma=10$, $\rho=28$, and $\beta=8/3$, the system exhibits chaotic behavior. Figure 1 illustrates the Lorenz signal in the *x* (vertical) direction, which describes the convection intensity of the atmosphere. All the operations investigated here are applicable to the Lorenz signal in other two directions. Figure 2 illustrates the effect of adding white noise to reduce the signal-to-noise ratio (SNR) to 20 dB. After the LGP-based noise reduction approach is applied to the signal, SNR is improved by 10.3 dB, as shown in Fig. 3.

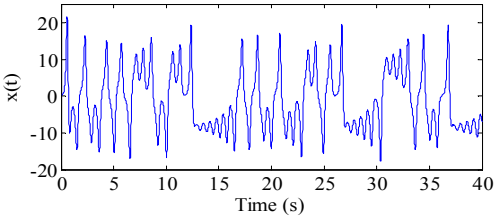

Fig. 1. Lorenz signal in x direction (noise free)

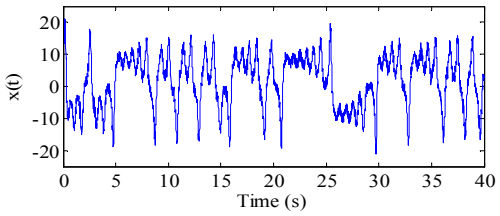

Fig. 2. Lorenz signal with additive white noise (SNR=20 dB)

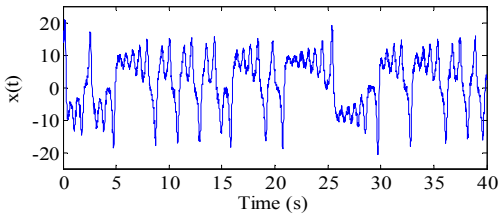

Fig. 3. Lorenz signal after noise reduction (SNR=30.3 dB)

Table I presents the results of further simulations with various levels of additive white noise. It is clear that LGP-based noise reduction approach was able to significantly improve Lorenz signals with very low initial SNR.

Table I. LGP noise reduction results under different SNRs

SNR		
Before LGP (dB)	**After LGP (dB)**	**Improvement (dB)**
1	5.1	4.1
3	7.2	4.2
6	11.4	5.4
10	15.6	5.6
15	24.6	9.6
20	30.3	10.3

Synthetic Signal

To simulate vibration signals from a rolling bearing with embedded defects, a synthetic signal was formulated. Generally, signals from a bearing may include: 1) vibration with a characteristic frequency of f_u equal to the bearing rotational speed, caused by bearing unbalance in which the gravitational center of the bearing does not coincide with its rotational center; 2) vibration at frequency f_m, equal to twice the shaft speed caused by bearing misalignment in which the two raceways of the bearing (inner and outer) do not lie in the same plane, so that the raceway axis and the axis of the rotating shaft are not parallel; 3) vibration at the frequency f_{BPFO} due to rolling elements periodically passing over a fixed reference position on the outer raceway, , and, 4) structure-borne vibration which is broad-band and can be modeled as white noise.

When a localized structural defect occurs on the surface of the bearing raceways (inner or outer), a series of impacts will be generated every time the rolling elements collide with the defects. Such forced vibration is represented by high frequency bursts that are amplitude-modulated at the repetition frequency of the impacts. In the numerical simulation, only defect-

induced resonant vibrations and structure-borne vibrations are considered, as other vibration components can be filtered out through signal pre-processing. Defect-induced resonant vibration was simulated as a periodic Gaussian pulse signal as shown in Fig. 4. The pulse repetition frequency is 50 Hz, the sampling rate is 20 kHz, and pulse train length is 200 ms.

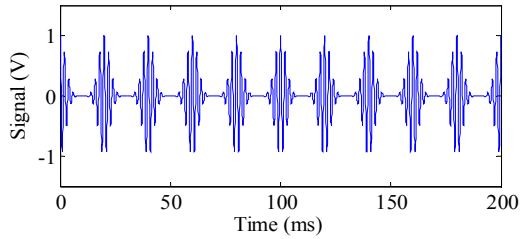

Fig. 4. Simulated defect-induced resonant vibrations

To include the effects of structure-borne vibration, white noise was added to the signal of Fig. 4 to reduce the SNR to 4 dB. The resulting signal is shown in Fig. 5.

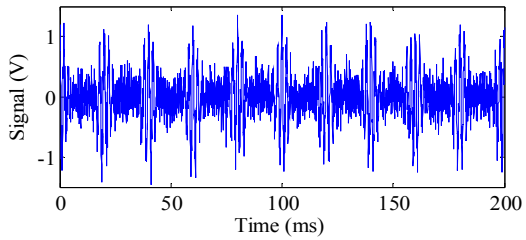

Fig. 5. The synthetic signal before noise reduction

After the LGP algorithm was applied to reduce the noise of the synthetic signal, the Gaussian pulses could be clearly identified, as shown in Fig. 6. The signal-to-noise ratio was improved to reach 10 dB.

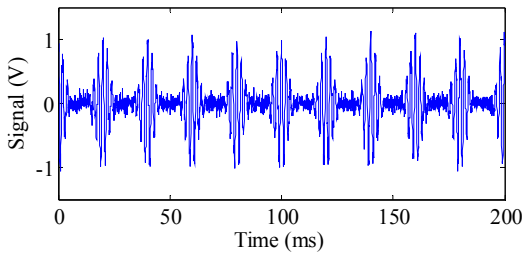

Fig. 6. The synthetic signal after noise reduction

IV. EXPERIMENTAL VERIFICATION

In the experiment with a pair of rolling element bearings (type 6205), one bearing had no known defects, and the other had a 0.1 mm-wide groove across its outer raceway. Vibration signals were measured for 1,440 rpm shaft speed with a sampling frequency at 12,800 Hz. Figure 7 illustrates the waveforms of the measured signals.

The results of applying the LGP algorithm to the two vibration signals are shown in Fig. 8. Close inspection reveals that the amplitudes of the baseline noise envelopes are smaller in Fig. 8 than that in Fig. 7. Further processing was done by calculating the multi-fractal spectrum [6] of each signal. The multi-fractal spectrum is a nonlinear time series analysis technique for characterizing the distribution of singularities of a signal. Generally, changes in the singularity distribution of the signal indicate variations of the characteristics of the signal, which is often caused by changes in a bearing's operation condition. To quantitatively utilize the multifractal spectrum [denoted as $h \sim D(h)$] information, the width of the multi-fractal spectrum (Δh) which is defined as $\Delta h = h_{max} - h_{min}$, with $D(h_{max}) = D(h_{min}) = 0$, and depicts the degree of singularity distribution of a signal is extracted for bearing defect identification.

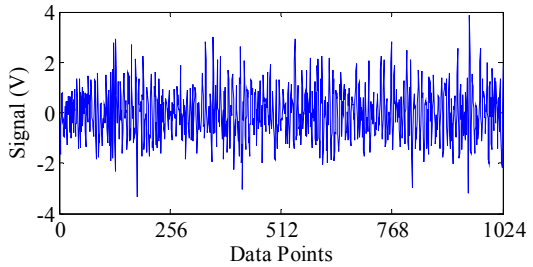

(a) Signal from a bearing without defect

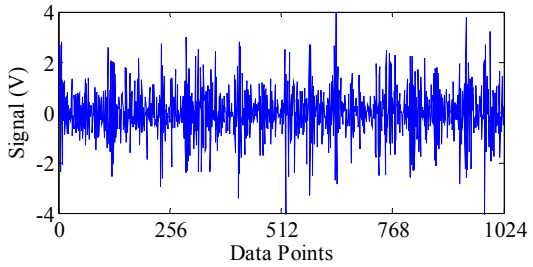

(b) Signal from a defective bearing

Fig. 7. Vibration signals measured from the test bearings before noise reduction

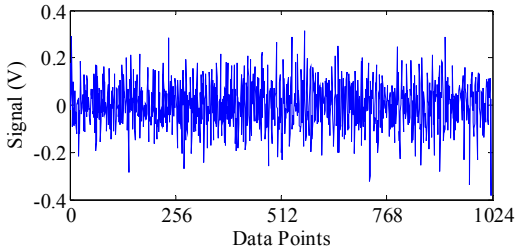

(a) Signal from a bearing without defect

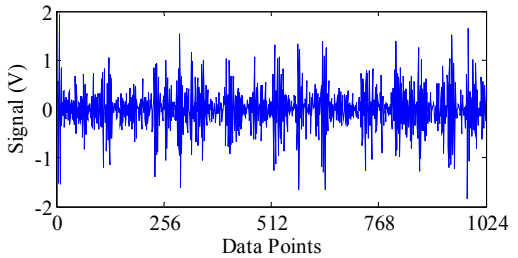

(b) Signal from a defective bearing

Fig. 8. Vibration signals measured from the test bearings after noise reduction

For purpose of comparison, Figures 9 and 10 illustrate the multi-fractal spectra for both bearings before and after noise reduction. The multi-fractal spectrum of the LGP-processed signal from the defective bearing is wider than that of the

healthy bearing. This can be explained by the presence of additional frequency components (due to defect-induced vibrations) in the vibration signal from a defective bearing and the consequent lower regularity of the signal, and wider singularity distribution. Furthermore, the difference of the widths of the multi-fractal spectra for the healthy and defective bearings after LGP-based noise reduction is larger than that before noise reduction (18% vs. 7.8%), as listed in Table II. This indicates the effectiveness of the LGP-based noise reduction for improving bearing defect identification.

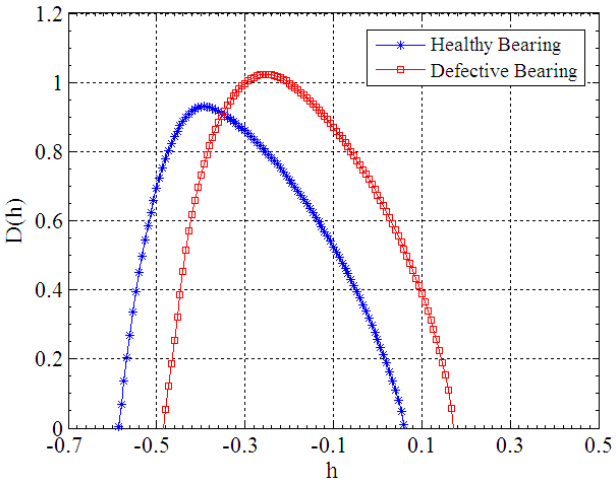

Fig. 9. Multi-fractal spectra of the bearing vibration signals before noise reduction

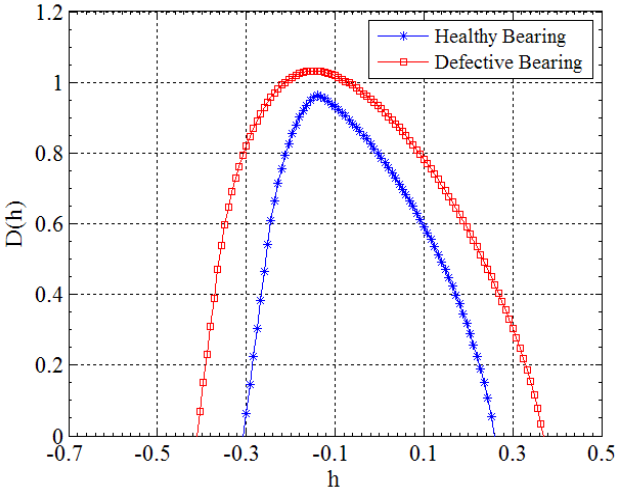

Fig. 10. Multi-fractal spectra of the bearing vibration signals after noise reduction

Table II. Multi-fractal spectrum parameters for test bearings

Bearing	Δh *(Before noise reduction)*		Δh *(After noise reduction)*	
Healthy	0.634	7.8%	0.582	18%
Defective	0.683		0.687	

V. CONCLUSION

The effectiveness of a local geometric projection-based technique for improving signal-to-noise ratio in dynamical signal decomposition and feature extraction is demonstrated. Different levels of white noise were added to a Lorenz signal to investigate the effectiveness of the noise reduction technique. The results indicate that the LGP-based technique is robust where nonlinear behavior exists. Analysis of both simulated and experimental bearing vibration signals further demonstrated that LGP-based signal processing is a viable tool for machine condition monitoring and health diagnosis.

ACKNOWLEDGMENTS

This work was supported by the Advanced Manufacturing Systems Program at the National Institute of Standards and Technology (NIST).

REFERENCES

[1] Comparin, R.J. and Singh, R., 1990, “An Analytical Study of Automotive Neutral Gear Rattle”, Journal of Mechanical Design, 112, pp. 237-245.

[2] Ghafari, S.H., Golnaraghi, F., and Ismail F., 2007, “Effect of Localized Faults on Chaotic Vibration of Rolling Element Bearings”, Nonlinear Dynamics, DOI 10.1007/s11071-007-9314-2.

[3] Muller, P.C., Bajkowski, J., and Doffker, D., 1994, “Chaotic Motions and Fault Detection in a Cracked Rotor”, Nonlinear Dynamics, 5, pp. 233-254.

[4] Logan, D. and Mathew, J., 1996, “Using the Correlation Dimension for Vibration Fault Diagnosis of Rolling Element Bearing: Basic concepts”, Mechanical Systems and Signal Processing, 10, pp. 241-250.

[5] Jiang, J.D., Chen, J., and Qu, L.S., 1999, “The Application of Correlation Dimension in Gearbox Condition Monitoring”, Journal of Sound and Vibration, 223(4), pp. 529-541.

[6] Yan, R. and Gao, R., “Wavelet-Based Multi-fractal Spectrum for Machine Defect Identification”, ASME Conference on International Mechanical Engineering Congress and Exposition, Paper No. 41984, Seattle, WA, November 11-15, 2007.

[7] Tao, X., Du, B., and Xu, Y., 2007, “Bearing Fault Diagnosis Based on GMM Model Using Lyapunov Exponent Spectrum”, Proceedings of 33rd Annual Conference of the Industrial Electronics Society, Nov. 5-8, pp. 2666-2671.

[8] Kostelich, E. J. and Schreiber, T., 1993, “Noise Reduction in Chaotic Time Series Data: A Survey of Common Methods”, Physical Review E, 48(3), September, pp. 1752-1763.

[9] Kantz, H. and Schreiber T., 1997, Nonlinear Time Series Analysis, Cambridge University Press, UK.

[10] Kostelich, E. J. and Yorke J.A., 1988, "Noise Reduction in Dynamics Systems", Physical Review A, 38(3), pp. 1649-1952.
[11] Hammel, S.M., 1990, "A Noise Reduction Method for Chaotic System", Physics Letter A, 148(8,9), pp. 421-428.
[12] Farmer, J.D. and Sidorowich, J.J., 1991, "Optimal Shadowing and Noise Reduction", Physica D, 47(30), pp. 373-392.
[13] Schreiber, T., 1993, "Extremely Simple Nonlinear Noise-Reduction Method", *Physical Review E*, 47(4), April, pp. 2401-2404.
[14] Cawley, R. and Hsu, G. H., 1992, "Local Geometric Projection Method for Noise Reduction in Chaotic Maps and Flows", Physical Review A, 46(6), September, pp. 3057-3082.
[15] Urbanowicz, K. and Holyst, J, A., 2004, "Noise Reduction in Chaotic Time Series by a Local Projection with Nonlinear Constraints", Acta Physica Polonica B, 35(9), pp. 2175-2197.
[16] Leontitsis, A., Bountis, T., and Pagge, J., 2004, "An Adaptive Way for Improving Noise Reduction Using Local Geometric Projection", *Chaos*, 14(1), March, pp. 106-110.
[17] Signorini, M. G., Marchetti, F., and Cerutti, S., 2001, "Applying Nonlinear Noise Reduction in the Analysis of Heart Rate Variability", IEEE Engineering in Medicine and Biology Magazine, 20(2), March/April, pp. 59-68.
[18] Sun, J., Zheng, N., and Wang, X., 2007, "Enhancement of Chinese Speech Based on Nonlinear Dynamics", Signal Processing, 87, pp. 2431-2445.
[19] Wang, F., Wang, Z., and Gao J., 2002, "Extracting Weak Harmonic Signals From Strong Chaotic Interference", Circuits Systems Signal Processing, 21(4), pp. 427-448.
[20] Takens, F. 1981, "Detecting Strange Attractors in Turbulence", Dynamical Systems and Turbulence, Lecture Notes in Mathematics, Rand, D. A. and Young, L.S (Eds.), Springer-Verlag, Berlin, pp. 366–381.
[21] Fraser, A.M. and Swinney H.L., 1986, "Independent Coordinates for Strange Attractors from mutual information", Physical Review A, 33, pp. 1134-1140.
[22] Grassberger, P. and Procaccia, I., 1983, "Measuring the Strangeness of Strange Attractors", Physica D, 9, pp.189-208.
[23] Kennel, M.B., Brown, R., and Abarbanel, H.D., 1992, "Determining Embedding Dimension for Phase-Space Reconstruction Using a Geometrical Construction", Physical Review A, 45(6), pp.3403-3411.
[24] Kim, H.S., Eykholt, R., and Salas, J.D., 1999, "Nonlinear Dynamics, Delay Times and Embedding Windows", Physica D, 127, pp. 48-60.
[25] Lorenz, E. N.,1963, "Deterministic Nonperiodic Flow", Journal of the Atmospheric Sciences, 20, pp.130-141.